Development/Plasticity/Repair

Dynamic Regulation of Synaptic GABA Release by the Glutamate-Glutamine Cycle in Hippocampal Area CA1

Shu-Ling Liang,[1] **Gregory C. Carlson,**[1] **and Douglas A. Coulter**[1,2]

[1]Division of Neurology and the Pediatric Regional Epilepsy Program, Children's Hospital of Philadelphia, and [2]Departments of Pediatrics, Neurology, and Neuroscience, University of Pennsylvania School of Medicine, Philadelphia, Pennsylvania 19104

Vesicular GABA and intraterminal glutamate concentrations are in equilibrium, suggesting inhibitory efficacy may depend on glutamate availability. Two main intraterminal glutamate sources are uptake by neuronal glutamate transporters and glutamine synthesized through the astrocytic glutamate-glutamine cycle. We examined the involvement of the glutamate-glutamine cycle in modulating GABAergic synaptic efficacy. In the absence of neuronal activity, disruption of the glutamate-glutamine cycle by blockade of neuronal glutamine transport with α-(methylamino) isobutyric acid (MeAIB; 5 mM) or inhibition of glutamine synthesis in astrocytes with methionine sulfoximine (MSO; 1.5 mM) had no effect on miniature IPSCs recorded in hippocampal area CA1 pyramidal neurons. However, after a period of moderate synaptic activity, application of MeAIB, MSO, or dihydrokainate (250 μM; an astrocytic glutamate transporter inhibitor) significantly reduced evoked IPSC (eIPSC) amplitudes. The MSO effect could be reversed by exogenous application of glutamine (5 mM), whereas glutamine could not rescue the eIPSC decreases induced by the neuronal glutamine transporter inhibitor MeAIB. The activity-dependent reduction in eIPSCs by glutamate-glutamine cycle blockers was accompanied by an enhanced blocking effect of the low-affinity GABA$_A$ receptor antagonist, TPMPA [1,2,5,6-tetrahydropyridin-4-yl)methylphosphinic acid], consistent with diminished GABA release. We further corroborated this hypothesis by examining MeAIB effects on minimal stimulation-evoked quantal IPSCs (meIPSCs). We found that, in MeAIB-containing medium, moderate stimulation induced depression in potency of meIPSCs but no change in release probability, consistent with reduced vesicular GABA content. We conclude that the glutamate-glutamine cycle is a major contributor to synaptic GABA release under physiological conditions, which dynamically regulates inhibitory synaptic strength.

Key words: GABAergic modulation; hippocampus; neurotransmitter; interneuron; astrocyte; astroglia; glutamate transporters; synaptic transmission; GABA; glutamine; patch clamp; unitary

Introduction

Synaptic vesicle content at equilibrium reflects the dynamics of filling and leak, both of which depend on the concentration of neurotransmitter (for review, see Williams, 1997; Axmacher et al., 2004). Depleting or enhancing intraterminal cytoplasmic concentrations of neurotransmitter would therefore be expected to decrease or enhance vesicle content, respectively, as has been observed experimentally in various synapses (Murphy et al., 1998; Pothos et al., 1998), including hippocampal inhibitory synapses (Engel et al., 2001; Sepkuty et al., 2002; Mathews and Diamond, 2003). A recent study consistent with this idea demonstrated that GABA vesicle content is in dynamic equilibrium with intraterminal glutamate concentrations (Mathews and Dia-

mond, 2003). Although interneurons do recycle GABA from the synaptic cleft through GABA transporters, the principal source of GABA packed into synaptic vesicles is derived from decarboxylation of glutamate by glutamic acid decarboxylase (GAD) (Martin and Tobin, 2000).

There are two primary sources for this glutamate in interneurons. One is glutamate uptake via glutamate transporters [excitatory amino acid carrier 1 (EAAC1)] located in the presynaptic terminals of GABAergic neurons (Kanai and Hediger, 1992; Arriza et al., 1994; Bjoras et al., 1996; Nakayama et al., 1996; Velaz-Faircloth et al., 1996; Eskandari et al., 2000). A second source of glutamate is derived from the astrocytic glutamate-glutamine cycle, where glutamate is taken up by astrocytes through the astrocyte-specific glutamate transporter-1 (GLT-1) and converted into glutamine by glutamine synthetase (Pines et al., 1992; Arriza et al., 1994). Glutamine is then released from astrocytes by system N transporters and transferred into neurons by system A transporters (Chaudhry et al., 2002a). In neurons, glutamine is converted into glutamate by glutaminase. Glutamate is decarboxylated to generate GABA and is subsequently packaged into vesicles (summarized in Fig. 2F). Data from a recent study revealed that disrupting the glutamate-glutamine cycle reduces hippocampal GABA neurotransmitter pools (Rae et al., 2003). Furthermore, glutamine synthetase expression is significantly de-

creased in the human epileptic hippocampus (Eid et al., 2004). Combined, these data indicate that the glutamate-glutamine cycle may play a role in regulation of inhibitory synaptic strength, which can influence circuit excitability under normal and pathological conditions.

In the present study, we demonstrate that, under low-activity conditions, disruptions of the endogenous glutamine supply by blockade of neuronal glutamine transport or inhibition of astrocytic glutamine synthesis has no significant effect on miniature IPSC (mIPSC) amplitudes. However, after elevating inhibitory synaptic activity to more physiological levels, we found that pharmacological interruption of the glutamine supply significantly decreased both evoked IPSC (eIPSC) and minimal stimulation-evoked quantal IPSC (meIPSCs) amplitudes by reducing the amount of GABA released at individual synapses. Exogenous application of glutamine reversed eIPSC decreases induced by astrocytic glutamine synthesis inhibitors but not neuronal glutamine transporter inhibitors, consistent with a role for the glutamate-glutamine cycle in modulating local neuronal GABA synthesis and packaging of neurotransmitter into vesicles. Based on these findings, we conclude that the glutamate-glutamine cycle is a major contributor in the maintenance of synaptic GABA release, and that alterations in the efficacy of this cycle may modulate GABAergic synaptic strength in an activity-dependent manner.

Materials and Methods

Slice preparation. Adult male Sprague Dawley rats (at least 6 weeks of age) were anesthetized with halothane before decapitation, in accordance with protocols approved by The Children's Hospital of Philadelphia Animal Care and Use Committee. The rat brain was rapidly removed from the skull after decapitation. Coronal hippocampi slices (350 μm) were prepared using a vibratome (VT1000S; Leica, Deerfield, IL) in ice-cold sucrose solution, in which NaCl in the artificial CSF (ACSF) was replaced by an equal osmolarity concentration of sucrose. The ACSF composition was as follows (in mM): 130 NaCl, 3 KCl, 1.25 NaH$_2$PO$_4$, 26 NaHCO$_3$, 10 glucose, 1 MgCl$_2$, 2 CaCl$_2$ (saturated with 95% O$_2$-5% CO$_2$). Slices were then incubated at 34°C for 30 min and then allowed to recover for at least 1 h at room temperature before experimentation. For studies involving inhibition of glutamine synthetase, methionine sulfoximine (MSO; 1.5 mM) was included in the ACSF solution used for preincubation. The osmolarity of all solutions used was 305–315 mOsm.

Experimental setup for visualized patch-clamp recording and laser photolytic release of caged GABA. A fixed stage upright microscope (Leica DMLFSA) with a 63× water immersion objective, equipped with a CCD camera (#C5985; Hamamatsu, Shizuoka, Japan) was used. Slices were maintained at 34°C, and gravity superfused with ACSF solution containing 6, 7-dinitroquinoxaline-2, 3-dione (DNQX; 10 μM) and D-(-)-2-amino-5-phosphonopentanoic acid (D-AP-5; 50 μM) to block glutamatergic responses. For studies involving inhibition of astrocytic glutamate transport, (S)-α-methyl-4-carboxyphenylglycine (MCPG; 50 μM) and (RS)-α-methylserine-O-phosphate (MSOP; 100 μM) were included in the ACSF solution to antagonize group I and III metabotropic glutamatergic receptors (mGluRs), which could be activated by elevated ambient glutamate levels under these conditions.

mIPSC recording. mIPSCs were recorded in ACSF that, along with DNQX and D-AP-5, included tetrodotoxin (TTX; 400 nM) to block action potentials. Whole-cell voltage-clamp recording of mIPSCs was conducted using a high-chloride internal pipette solution (E_{GABA} = −22 mV), which resulted in an inward chloride current when cells were clamped at −76 mV (corrected for junction potential). The pipette solution consisted of the following (in mM): 100 CsCH$_3$O$_3$S, 50 CsCl, 3 KCl, 0.2 BAPTA, 10 HEPES, 1 MgCl$_2$, 2.5 Phosphocreatine-2Na, 2 Mg-ATP, and 0.25 GTP-Tris, titrated to pH 7.2–7.3 with 3 M CsOH (osmolarity 280–290 mOsm). In all experiments, lidocaine N-ethylbromide (QX-314; 5 mM) was added to the pipette solution on the day of the experi-

ment. Synaptic currents were recorded using an Axopatch 200B amplifier (Molecular Devices, Sunnyvale, CA), filtered at 2 kHz, sampled at 10 kHz, digitized (Digidata 1320A; Molecular Devices), and stored for off-line analysis (using Minianalysis software written in IGOR Pro; Wavemetrics, Lake Oswego, OR) (Hwang and Copenhagen, 1999). Access resistance stability (10–18 MΩ; 80% compensation) was monitored using a +2 mV voltage step applied every 120 s, and data from cells were discarded when >15% change occurred.

Spontaneous IPSC, eIPSC, and meIPSC recording. Whole-cell voltage-clamp recordings of spontaneous IPSCs (sIPSCs), eIPSCs, and meIPSCs were conducted using a patch pipette containing one of the following solutions (in mM): 145 K-gluconate, 2 MgCl$_2$, 0.1 BAPTA, 2.5 KCl, 2.5 NaCl, 10 HEPES, 0.5 GTP-Tris, and 2 Mg-ATP, titrated to pH 7.2–7.3 with 1 M KOH, osmolarity 280–290 mOsm (V_{hold} = −27 mV); or alternatively, the same solution as the one used for mIPSCs (V_{hold} = −76 mV). eIPSCs were evoked using 100 μs constant-current bipolar stimulation (Stereotrode Tungsten, World Precision Instruments, Sarasota, FL; Isolator 10, Molecular Devices). The same electrode was used to generate the 15 min moderate stimulation protocol described in the Results. *In vivo* interneuron sleep and wake activity patterns were recorded from the unanaesthetized rat hippocampal CA1 region by Dr. Gyorgy Buzsaki (Rutgers University, Newark, NJ). Sleep and wake states were determined by observation of animal behavior and also by EEG rhythms.

Isolation of meIPSCs. meIPSCs were evoked from stratum radiatum via monopolar stimulation through an ACSF-filled patch electrode, placed 20–50 μm from the CA1 pyramidal cell body layer. The stimulating electrode position usually required adjustment to isolate meIPSCs. Three criteria were set for determination that meIPSCs were isolated: (1) events must be all or none and exhibit failures, (2) events were required to be similar in size to mIPSCs in CA1 pyramidal cells (20–50 pA) (compare Fig. 1), and (3) the synapses stimulated by the minimal stimulation were required to be part of the set of synapses generating the eIPSCs and therefore activated by the patterned stimulation. To produce an all or none response, stimulation intensity was titrated between 10 and 20 μA to generate a set response that had ~50% success rate (see Fig. 6A). Stimulation in stratum radiatum generated events very similar in size to the mIPSCs recorded in the same conditions plus TTX and allowed us to avoid the large meIPSCs, which were evoked, presumably from basket cells, by minimal stimulation in the cell body layer (Lambert and Wilson, 1994). Because of the small size of our events, it is likely that our location in stratum radiatum biased our selection toward dendritically targeted GABAergic terminals making one or a few synapses on the recorded cell, although it is also possible that we were selecting cut axons, isolating synapses from more profusely targeted GABAergic synapses such as those found with basket cells. To test that a minimally evoked synapse was also activated during the large evoked compound IPSC, the failure rate of meIPSCs was assessed, in isolation and 100 ms after an eIPSC. Overlapping activation of the meIPSC and eIPSC stimuli was confirmed by a large decrease in proportional success rate in evoking meIPSCs when preceded by an eIPSC (as shown in Fig. 6B). This demonstrated convergence of the larger bipolar and the minimal evoked stimulation.

Laser photolysis experiments. UV light for uncaging was generated by an argon ion laser (Coherent Enterprise II, Santa Clara, CA). UV light was delivered to the objective plane of the microscope by a multimode quartz optical fiber (Prairie, Madison, WI) and relayed through the 63× water-immersion objective to form an uncaging spot ~5 μm in diameter. This spot was targeted perisomatically on the recorded cell and adjusted to produce the largest response. The laser was gated to produce 1 ms duration laser uncaging pulses, which was used in all studies. To examine responses to GABA uncaging, recorded neurons were held at −27 mV, and uncaging pulses were delivered at 20 s intervals. The elicited GABA response amplitudes at CA1 pyramidal neurons were similar with no decrement over 10 events at this GABA uncaging interval. Throughout uncaging experiments, the recording chamber was connected to an oxygenated, continuously recycling 10 ml reservoir, which was used to administer the trifluoroacetic acid salt of α-carboxy-2-nitrobenzyl ester caged GABA (CNB-caged GABA). Solutions containing the caged compound were identical to those used for recording eIPSCs.

Data analysis. Data are expressed as mean ± SEM, and *p* values are derived from Student's paired *t* test, with significance levels assessed at $p < 0.05$. The sIPSC and mIPSC amplitude cumulative probability distributions were created either from control or treated cell responses, which were divided into 25 equal bins.

Drugs. DNQX, D-AP-5, MCPG, SR 95531 hydrobromide (gabazine), and MSOP were obtained from Tocris Cookson (Bristol, UK). TTX, α-(methylamino) isobutyric acid (MeAIB), histidine, MSO, dihydrokainate (DHK), (1,2,5,6-tetrahydropyridin-4-yl)methylphosphinic acid (TPMPA), QX-314, and glutamine were purchased from Sigma (St. Louis, MO). CNB-caged GABA was obtained from Invitrogen (San Diego, CA).

Results

Neither glutamine transporter blockade nor glutamine synthetase inhibition significantly affected mIPSC amplitudes

Because vesicular GABA concentrations are in equilibrium with synaptic terminal glutamate concentrations (Mathews and Diamond, 2003), if endogenous glutamine provided by the astrocytic glutamate-glutamine pathway is a critical source of the GABA substrate glutamate, then blockade of either neuronal glutamine uptake or astrocytic glutamine synthesis would rapidly result in the appearance of depleted or partially filled GABA synaptic vesicles. To begin to test this hypothesis, the amplitude of spontaneous GABAergic synaptic events produced in the presence of TTX to block action potential firing (mIPSCs) were used as an assay of vesicle content. We applied either an antagonist of the neuronal glutamine transporter (system A transporter), MeAIB (5 mM; applied acutely allowing for comparison of control and MeAIB exposed conditions), or a glutamine synthesis inhibitor, MSO (1.5 mM; preincubated in slices for at least 2–6 h), and compared mIPSCs recorded in the presence of these antagonists to those recorded in control conditions (Fig. 1*A*). Because mIPSCs are primarily quantal, if these antagonists had a significant effect on mIPSC amplitude, it would suggest that the astrocytic glutamate-glutamine cycle may have a constitutive role in GABA vesicle refilling. However, neither bath application of MeAIB (Fig. 1), nor preincubation with MSO altered median mIPSCs amplitudes compared with controls (Fig. 1*B*,*C*) ($p = 0.31$ for MeAIB, $n = 8$ cells, $p = 0.58$, 31.2 ± 2.3 pA for control, $n = 8$ cells compared with 29.5 ± 1.6 pA for MSO, $n = 7$ cells; data not shown). These results suggest that, under conditions in which cell firing is blocked, neither glutamine uptake into neurons nor glutamine generated by the astrocytic glutamate-glutamine cycle contribute to maintaining internal vesicle concentrations of GABA.

Effects of increasing activity levels on eIPSC amplitude

However, in contrast to the mIPSC recording conditions in which cell firing is blocked, GABAergic neurons can exhibit significant spontaneous activity, often firing bursts at frequencies ranging from 4 to 200 Hz, depending on behavioral state (Bartos et al., 2002; Klausberger et al., 2003). At these levels of activity, GABAergic vesicles are continually being released, recycled, and refilled, requiring additional transmitter. Because GABA reuptake constitutes only a minor source of vesicular neurotransmitter, intraterminal glutamate concentration may become limiting in response to net GABA efflux (Mathews and Diamond, 2003). Is it possible, under these more physiologically relevant rates of activity, that glutamine could become a significant substrate for synthesis of vesicular GABA? To assess this, our first experimental manipulation was to increase GABAergic neuronal activity using a moderate, repetitive burst stimulation protocol (four pulse 50 Hz bursts repeated at 20 s intervals, 0.05 Hz, for 15
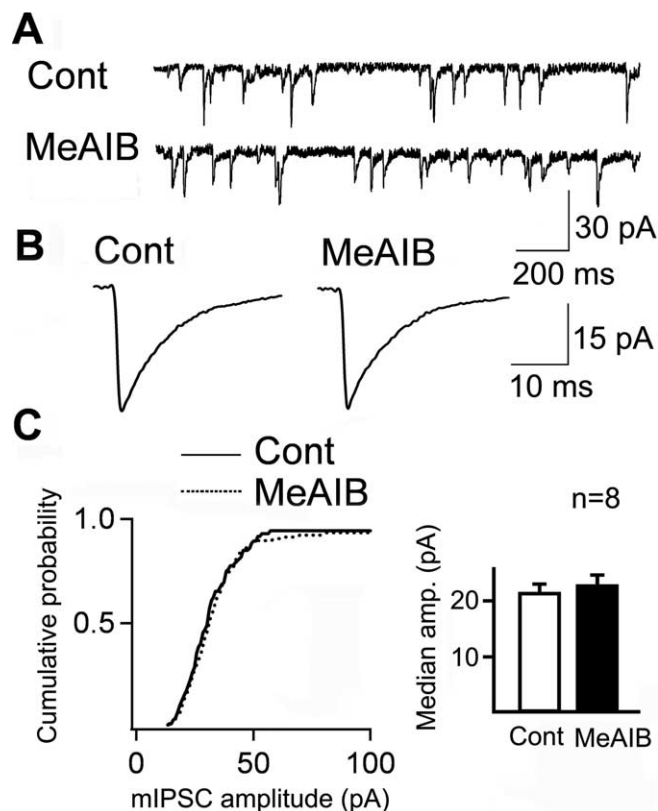
Figure 1. Application of the neuron-specific System A transporter inhibitor MeAIB does not change mIPSC amplitude. *A*, *B*, This is illustrated by the representative traces comparing mIPSC recorded in control (Cont) conditions to mIPSC recorded after application of MeAIB (5 mM; *A*) and averaged mIPSCs under each condition from the same cell (147 and 228 events in control and in the presence of MeAIB, respectively; *B*). *C*, Cumulative distribution of the same mIPSC events averaged in *B* show no effect of 5 mM MeAIB in these minimal activity conditions. The bar graph in *C* plots mean median mIPSC amplitudes (amp.) for eight cells under control (open bar) and MeAIB-exposed (filled bar) conditions, demonstrating no effect of MeAIB on mIPSC amplitudes.

min). As a control, a 15 min train of single stimuli at 0.05 Hz was used. eIPSCs were recorded before and after either a train of single or burst stimuli. Interestingly, the burst stimulation protocol itself significantly increased the peak amplitude of eIPSCs (Fig. 2*A*) (recorded within 5 min of termination of the burst protocol, to $163 \pm 24\%$ of preburst stimulation; $p < 0.01$, 414.8 ± 63 pA vs 580.1 ± 87.2 pA, prestimulation and poststimulation, respectively; $n = 16$). This potentiation was transient, gradually returned to the baseline within 30 min (to $99 \pm 8.5\%$ of preburst stimulation; $n = 6$) (Fig. 2*A*, iiii). The eIPSC enhancement was a specific response to the burst stimulation protocol; there was no change in eIPSC amplitude after 15 min of single stimuli at 0.05 Hz ($101 \pm 6.6\%$ of prestimulus amplitude; $p = 0.72$; 569.6 ± 153.2 vs 551.3 ± 124.5 pA, prestimulation and poststimulation, respectively; $n = 3$; data not shown). A similar long-term enhancement of eIPSCs has been reported in CA1 pyramidal cells after theta burst stimulation, which in many respects resembles our 15 min burst train (Perez et al., 1999).

Inhibition of neuronal glutamine uptake reduces eIPSC amplitude after burst stimulation

To test whether, after the period of moderate burst stimulation, glutamine was being used to generate GABA, the burst protocol was repeated in the presence of the glutamine transporter inhib-

itor MeAIB (5 mM). In contrast to the increase seen in eIPSC size after burst stimulation in control medium, in MeAIB, eIPSC amplitude was decreased after stimulation (Fig. 2B) (to 57 ± 6.7% of preburst stimulation, $p < 0.02$; 510.5 ± 90.5 vs 301.6 ± 68.0 pA, prestimulation and poststimulation, respectively, assessed within 5 min of termination of the burst protocol, here and in data described below; $n = 11$). In six additional cells, the broader spectrum glutamine transporter antagonist histidine (Rae et al., 2003) produced a similar magnitude effect to MeAIB on eIPSC size postburst stimulation (amplitude decreased to 62 ± 12% of preburst levels; $p < 0.03$; data not shown). The MeAIB-induced reduction in eIPSC amplitude was reversible, because it returned to baseline within 30 min (to 82 ± 11% of preburst stimulation; $n = 5$) (Fig. 2B). Apparently, in the absence of elevated activity, alternate sources of glutamate and GABA (such as neuronal uptake) may be sufficient to replenish vesicular GABA (Sepkuty et al., 2002; Mathews and Diamond, 2003), explaining recovery in the continued presence of antagonist. MeAIB had no effect on eIPSCs following single stimulation at 0.05 Hz for 15 min (103 ± 10% of prestimulus amplitude; $p = 0.8$; 572.9 ± 252.0 vs 560.1 ± 215.8 pA, prestimulation and poststimulation, respectively; $n = 3$; data not shown). These differences in eIPSC size after burst stimulation in the presence of neuronal glutamine uptake inhibitors suggested that, after periods of elevated activity, inhibitory synaptic efficacy is strongly dependent on endogenous neuronal (SA-1) glutamine transporter activity in GABAergic neurons.

Spontaneous IPSCs are not affected by moderate stimulation or MeAIB

During the course of moderate burst stimulation in the presence of MeAIB (described above), we also analyzed the amplitude of sIPSCs recorded simultaneously. Presumably, these sIPSCs represent activity in the majority of inhibitory synapses onto recorded neurons, a much larger synaptic population than the subset of activated synapses generating the eIPSCs. Because the stimulated synapses exhibited IPSC reductions, we hypothesized that, if this was specific to the activated terminals, alterations should be restricted to eIPSCs, and there should be little or no effect of MeAIB on sIPSCs. This was the case. Burst stimulation in the presence of MeAIB had no effect on sIPSC median amplitude ($p = 0.42$; $n = 6$ cells) (Fig. 2E). In this same set of six cells, eIPSC amplitude postburst was reduced to 62 ± 5% of preburst stimulation levels. These data demonstrate that the effect of MeAIB on eIPSC amplitudes is activity dependent and restricted to the stimulated synapses.
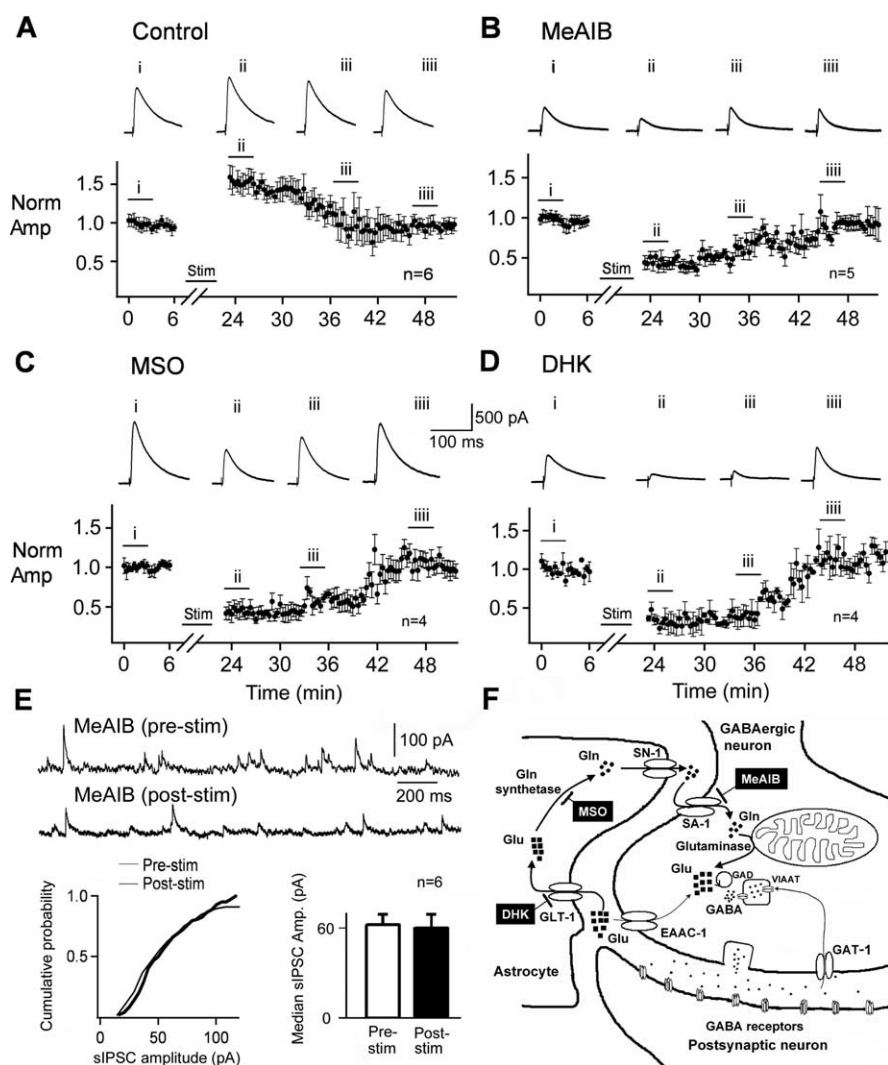

Figure 2. Moderate activity (15 min of 50 Hz, 4 pulse bursts 20 s apart) increased eIPSC amplitude in a glutamate-glutamine cycle-dependent manner. **A**, eIPSCs are increased after a 15 min period of moderate burst stimulation (stim). Plotted eIPSC amplitude averaged from a group of six recorded cells shows that, after the moderate stimulation, eIPSCs increase over control (**A**; and traces i and ii; i–iiii are representative traces from one cell averaged over the period indicated). This effect recovers to control levels after 25–30 min (iiii). **B–D**, Disruption of the glutamate-glutamine cycle reverses this effect, generating a reduction in eIPSCs when moderate stimulation is performed in the presence of the System A transport blocker MeAIB (5 mM; **B**), the glutamine synthetase inhibitor MSO (1.5 mM; **C**), or the astrocyte-specific glutamate uptake inhibitor DHK (250 μM; **D**). Comparing averaged traces (i and ii) from the representative cells in each inhibitor and group data (**B–D**) show a similar reduction from each blocker after stimulation despite their very different targets (illustrated in **F**). In all cases, the eIPSC reduction after stimulation recovered within 25–30 min (iiii in **B–D**). **E**, A similar reduction in IPSCs poststimulus was not seen in the sIPSCs in the presence of MeAIB, demonstrating that the reduction seen with the eIPSCs was dependent on an increase in synaptic activity. The bar graph in **E** depicts mean median sIPSC amplitude for six cells before and after burst stimulation. The event numbers in the cumulative frequency distribution are 194 prestimulation and 97 poststimulation. **F** shows the glutamine cycle through an astrocyte into a GABAergic neuron, starting from glutamate (Glu) uptake into an astrocyte via GLT-1 to glutamine (Gln) synthesis by Gln synthetase and then transport out of the astrocyte and into the GABAergic neuron by the System N (SN-1) and A (SA-1) transporters, respectively. Inside the terminal, Gln is returned to Glu by mitochondrial glutaminases, providing Glu for conversion to GABA by GAD for transport into synaptic vesicles via the vesicular inhibitory amino acid transporter (VIAAT). The various targets for inhibition by MeAIB (**B**), MSO (**C**), and DHK (**D**) are indicated by a bar symbol.

Burst stimulation results in enhanced release probability of inhibitory synapses but no change in postsynaptic GABA receptor sensitivity

Multiple processes may be modulated by burst stimulation to transiently increase eIPSC size, and thus potentially could be interrupted by our pharmacological blockade of the glutamate-glutamine cycle. Therefore, we sought to identify the primary mechanisms underlying the burst stimulation-induced eIPSC
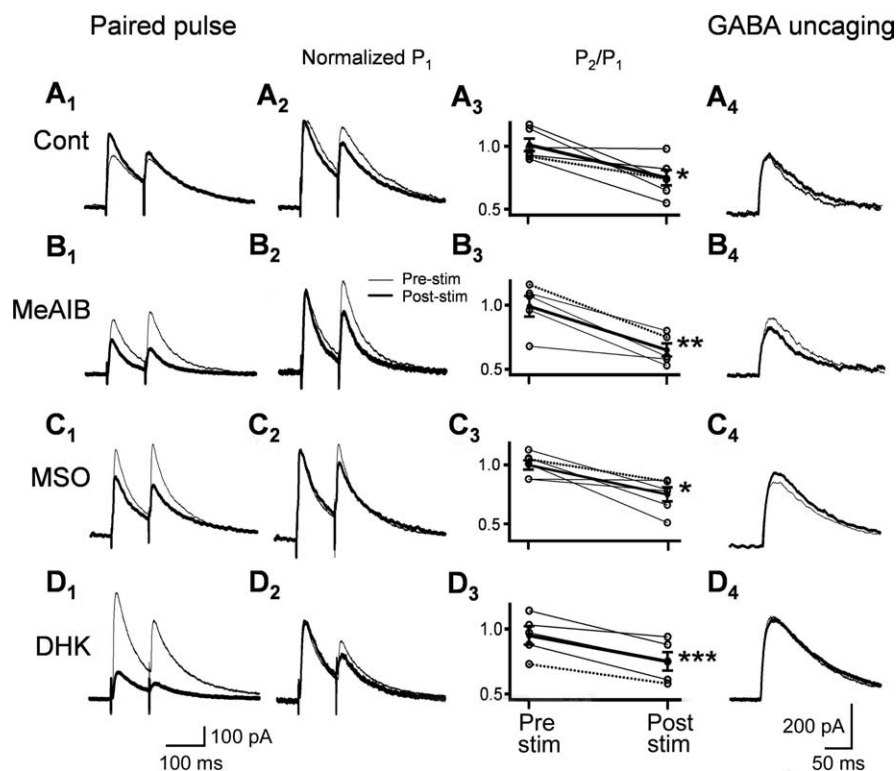
Figure 3. The eIPSC increase after moderate stimulation is attributable to, in part, increased release probability, an effect independent of the poststimulus eIPSC reduction caused by disruption of the glutamate-glutamine cycle. To assess changes in release probability, we performed paired-pulse stimulation before and after the moderate stimulation protocol. Under control conditions in **A**, the increase in amplitude (representative traces **A₁**; thick line) poststimulus over prestimulus conditions (thin line) is associated with an increase in probability of release. This is revealed when the traces are normalized (**A₂**) to the initial response (P_1), showing a relative decrease in the poststimuli response; this indicates increased release probability. This increase in release probability (decrease in P_2/P_1) was consistent, appearing in every cell tested (**A₃**; thin line and, from representative trace, dotted line) as well as on average (thick line). In the same cell from **A₁**, we elicited fast GABA responses with 1 ms local laser-induced release of CNB-caged GABA (250 μM) before (thin line) and after (thick line) stimulation and found no change in the representative cell (**A₄**), indicating that postsynaptic GABA receptor sensitivity was unchanged by the burst stimulus. Interestingly, this increase in release probability was maintained in the poststim condition when eIPSC amplitude was reduced by glutamate-glutamine cycle inhibitors (**B–D**). Despite the eIPSC decrease reflected by the poststimulus traces (**B₁–D₁**), the normalized representative traces (**B₂–D₂**) show a similar P_2 reduction in poststimulus conditions as found in control (**A₂**). This maintenance of increased release probability poststimulus is borne out in the group data, showing no difference on moderate stimulation effect on the P_2/P_1 ratio between control and in the presence of MeAIB, MSO, or DHK (**A₃–D₃**). Similarly, from photo-uncaging of GABA, there appeared to be no change in GABA receptor sensitivity from either preburst conditions or compared with control condition in MeAIB (**B₄**), MSO (**C₄**), and DHK (**D₄**). Statistical significance is indicated (*$p < 0.05$, **$p < 0.01$, ***$p < 0.005$).

enhancement in control medium shown in Figure 2A. We hypothesized that two likely candidate mechanisms could mediate this effect. First, release probability of GABA synapses could be enhanced, resulting in larger eIPSCs after stimulation. Second, increasing the level of GABAergic neuronal activity could enhance the sensitivity of postsynaptic GABA receptors, leading to a larger response to the evoked GABA release. To ascertain which of these mechanisms might contribute to the increase in eIPSC amplitude after burst stimulation, we conducted a set of studies in which we assessed changes in presynaptic release probability indirectly using paired-pulse stimulation and in the same cells tested postsynaptic GABA receptor sensitivity by measuring responses to laser uncaging of GABA. As in the eIPSC studies, preburst and postburst stimulation responses were compared. Results from these studies demonstrated that, after burst stimulation in control medium, the increase in eIPSC amplitude was associated with an increase in paired-pulse depression of eIPSCs (Fig. 3A₁, A₂); this is plotted in Figure 3A₃ [paired-pulse

ratio (PPR) is calculated from the average of 10 trials]. These results clearly showed enhanced paired-pulse depression in these synapses after the burst stimulation (decreased PPR to $75 \pm 6.9\%$ of prestimulation levels; $p < 0.02$; $n = 6$ cells). A decrease in PPR is usually considered to indicate the summed effect of an increase in probability of release, although other synaptic factors may be involved. To identify an actual change in probability of release, changes in the release rate of evoked unitary events can be assessed (see below).

In contrast, after the burst stimulation in the same cells, there was no evidence for the stimulation protocol increasing the sensitivity of postsynaptic GABA receptors. Responses to perisomatic laser uncaging of CNB-caged GABA (250 μM) were unchanged preburst and postburst stimulation (peak amplitude was $100 \pm 2.8\%$ of preburst levels; $p = 0.4$; 375.9 ± 129.7 vs 364.4 ± 117.9 pA, prestimulation and poststimulation, respectively; $n = 6$) (Fig. 3A₄). Although it was impossible to restrict GABA application to the subset of synapses that were stimulated during eIPSC studies, our data demonstrate that the increase in eIPSC size postburst stimulation is not a result of a more general, cell-wide increase in GABA receptor sensitivity or Cl⁻ driving force. Combined, these results suggest that the increase in eIPSC amplitude after the burst stimulation was attributable to, at least in part, enhanced presynaptic release probability and not to changes in the sensitivity of postsynaptic GABA receptors.

MeAIB-induced eIPSC reductions are not attributable to changes in PPR or postsynaptic GABA receptor sensitivity
Despite the significant decrease in eIPSC amplitude in MeAIB, the release probability of GABA synapses remained increased in response to the burst stimulation protocol (PPR decreased to $67 \pm 5.7\%$ of preburst stimulation; $p < 0.01$; $n = 5$ cells) (Fig. 3B₁–B₃), as was seen in control medium (Fig. 3A₃). Nor could the MeAIB associated decrease in eIPSC postburst stimuli be attributed to a global change in postsynaptic GABA sensitivity, because there was no change in the magnitude of the GABA uncaging response after burst stimulation in MeAIB (peak amplitude $105 \pm 10\%$ of preburst; $p = 0.3$; 282.7 ± 56.2 vs 301.5 ± 66.8 pA, prestimulation and poststimulation, respectively; $n = 4$) (Fig. 3B₄). Thus, it appeared likely that MeAIB, through its actions to block glutamine transport into GABAergic neurons, was reducing eIPSC amplitude by decreasing the amount of synaptic GABA release, without altering release probability or postsynaptic sensitivity. Next, we conducted additional studies to test the hypothesis that eIPSC reductions were a result of reduced glutamine flux via the astrocytic glutamate-glutamine cycle (illustrated in Fig. 2F).

Inhibition of astrocytic glutamine synthesis reproduces the effects of MeAIB

The most likely source of glutamine for transport into GABAergic neurons is from astrocytes. To determine whether this is the case under our experimental conditions, we tested the effect of an astrocytic glutamine synthesis inhibitor, MSO (1.5 mM), on eIPSCs. Because MSO needs to be taken into astrocytes to act, all slices were preincubated in ACSF containing MSO (1.5 mM) for 2–6 h before recording. Compared with the result obtained with MeAIB, MSO significantly reduced eIPSC size postburst (Fig. 2C) (to $68 \pm 6\%$ of preburst stimulation; $p < 0.0005$; 483.5 ± 48.9 vs 316.0 ± 39.2 pA, prestimulation and poststimulation, respectively; $n = 15$), eIPSC amplitude also returned to $107 \pm 14\%$ of baseline within 30 min ($n = 4$) (Fig. 2C) after burst stimulation. This decrease in eIPSC amplitude was highly specific to the activated synapses, because there was no significant change in median sIPSC amplitude after stimulation in the presence of MSO ($p = 0.75$; 54.8 ± 4.7 vs 53.1 ± 5.3 pA, preburst and postburst stimulation, respectively; $n = 7$ cells; data not shown). Moreover, as with MeAIB, in MSO, the decreased PPR in GABA synapses after burst stimulation seen in control studies was maintained (Fig. 3C_3) (to $75 \pm 5.7\%$ of preburst stimulation; $p < 0.03$; $n = 6$ cells), whereas the eIPSC amplitude was decreased (to $63 \pm 11\%$ of preburst stimulation in the subset of cells in which a paired pulse protocol was conducted, $p < 0.02$; $n = 6$) (Fig. 2C). There was no significant increase in the responses to GABA uncaging in the presence of MSO after burst stimulation ($117 \pm 8\%$ of preburst stimulation in uncaging-evoked response; $p = 0.2$; 366.7 ± 96.8 vs 407.5 ± 81.8 pA, prestimulation and poststimulation, respectively; $n = 4$) (Fig. 3C_4). Therefore, glutamine derived from astrocytic synthesis appears to be the primary source of glutamine supporting GABA synthesis in active GABA synapses.

Blockade of astrocytic glutamate uptake by DHK also induces activity-dependent eIPSC reductions

In the hippocampus, the astrocytic glutamate transporter is responsible for at least 80% of glutamate clearance and the majority of uptake-dependent synaptic inactivation (Bergles and Jahr, 1997; Danbolt, 2001). This glutamate, taken up by astrocytes via GLT-1, provides a significant source of the glutamate substrate in the glutamate-glutamine cycle. The data described above demonstrate that endogenous glutamine provided by astrocytes contributes to maintaining synaptic GABA release when GABAergic neuronal activity is enhanced. If this endogenous glutamine is synthesized from glial cytoplasmic glutamate originating from the astrocytic glutamate transporter, we expected that application of DHK would induce similar effects to MeAIB and MSO after burst stimulation. To test this hypothesis, we applied DHK (250 μM), together with MSOP (50 μM) and MCPG (100 μM) (mGluR I and III antagonists, respectively) during burst stimulation. mGluR antagonists were included in these experiments to prevent the effects of DHK-induced elevation of extracellular glutamate from acting on mGluRs located on GABA interneurons, which could confound our analyses (Huang et al., 2004). As shown in Figure 2D, the presence of DHK produced the same effects as MSO and MeAIB; the eIPSC amplitude was significantly decreased to $53 \pm 10\%$ ($p < 0.05$; from 360.2 ± 89.1 to 161.0 ± 31.8 pA; $n = 6$) but returned to $99 \pm 20\%$ of baseline within 30 min ($n = 4$). As with the other glutamate-glutamine cycle and glutamine transporter inhibitors, DHK application did not alter PPR postburst stimulation (Fig. 3D_1–D_3) (decreased PPR to $79 \pm 3.5\%$; $n = 5$; $p < 0.005$) nor change sensitivity to GABA uncaging relative to controls (peak amplitude, $98 \pm 10\%$ of preburst levels;
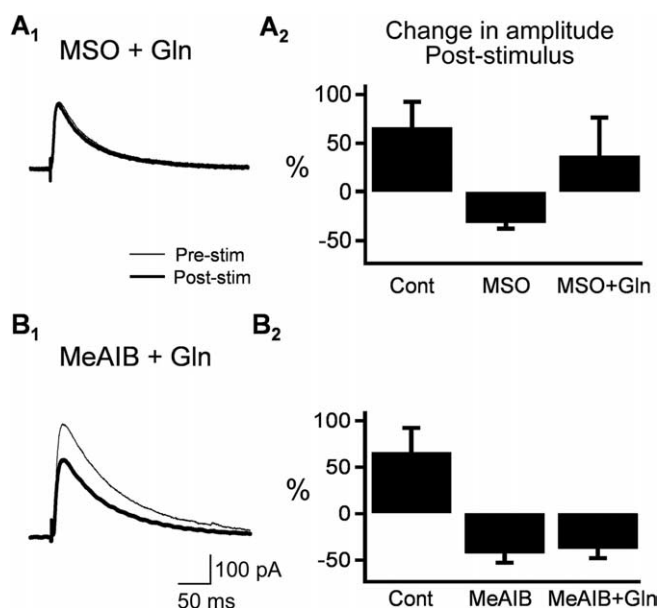

Figure 4. Poststimulation reduction of eIPSCs in MSO can be rescued by exogenous glutamine. Representative traces (A_1) show a small increase in eIPSC size in the presence of 1.5 mM MSO when glutamine is coapplied. This result is contrasted with peak amplitude decrease in MSO alone illustrated in A_2. Glutamine (5 mM) is ineffective in rescuing glutamine transport blockade by 5 mM MeAIB (B_1, B_2), confirming that in the MSO condition, exogenous glutamine is acting to replace the glutamine lost to reduced glutamine synthetase activity. Cont, Control; Pre-stim, prestimulation; Post-stim, poststimulation.

$p = 0.6$; 459.2 ± 83.8 vs 443.4 ± 77.9 pA, prestimulation and poststimulation, respectively; $n = 6$) (Fig. 3D_4). Thus, not only is glutamine generation via astrocytic glutamine synthetase able to modulate GABAergic efficacy, but this in turn depends on the ability of astrocytes to take up glutamate. Therefore, the availability of extrasynaptic glutamate may be a major determinate of GABAergic synaptic strength during periods of activity similar to that seen *in vivo*.

Reduction of eIPSCs by blocking glutamine synthesis is reversed by exogenous glutamine

The data presented in Figure 2 suggest that glutamine synthesis in astrocytes, its release, and transport into neurons are all required for localized GABA synthesis and maintenance of vesicle content in synapses following periods of sustained activity. If this was the case, we would expect that application of exogenous glutamine would reverse effects of inhibition of astrocytic glutamine synthesis by MSO but would be ineffective in reversing actions of the neuronal glutamine system A transporter blocker, MeAIB. Consistent with our hypothesis, the eIPSC amplitude reduction in MSO alone was reversed by simultaneous application of 5 mM glutamine and MSO to control postburst levels (peak amplitude increased to $137 \pm 39\%$ of preburst stimulation, from 334.5 ± 81.4 to 385.8 ± 95.4 pA; $n = 5$) (Fig. 4A_1,A_2). In contrast, when glutamine was applied together with the neuronal glutamine transport inhibitor MeAIB, there was no difference in stimulation-induced eIPSC amplitude effects when compared with MeAIB alone (decreased to $62 \pm 10\%$ of preburst stimulation, $p < 0.03$; from 379.6 ± 100.9 to 239.2 ± 59.9 pA; $n = 7$) (Fig. 4B_1,B_2). These results suggest that glutamine uptake into neurons was blocked by MeAIB, even when the concentration of extracellular glutamine was artificially high. We conclude from these results that astrocyte-synthesized glutamine serves as an
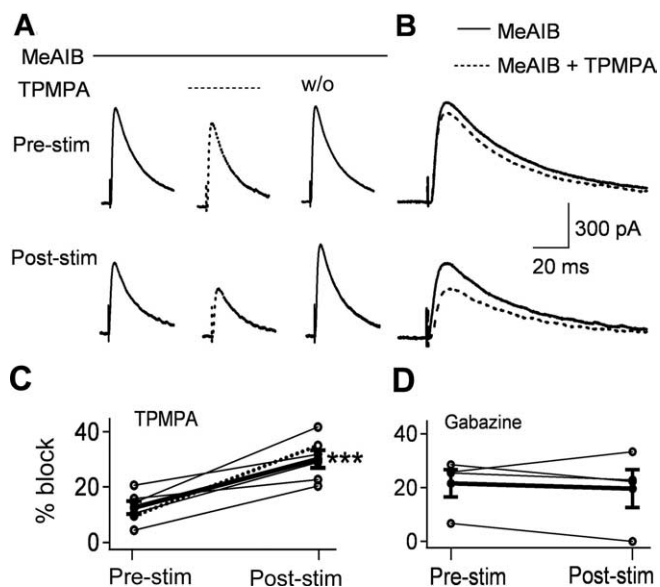
Figure 5. Consistent with a decrease in synaptic GABA release, a weak $GABA_A$ antagonist is more effective after moderate stimulation during glutamate-glutamine cycle disruption. The weak antagonist TPMPA was transiently applied before and after the moderate stimulus (**A**, **B**) at a concentration (30 μM) titrated to give a 10 –20% block of eIPSCs under control conditions; group data (**C**) demonstrate that TPMPA consistently and significantly had an increased antagonist effect on eIPSC amplitude, suggesting a decrease in GABA available to compete with TPMPA. In contrast, no change was seen when the high-affinity $GABA_A$ receptor antagonist gabazine (30 – 60 nM) was used at the same conditions of partial block (**D**). ***$p < 0.005$. Pre-stim, Prestimulation; Post-stim, poststimulation.

endogenous substrate that is transported into neurons and can dynamically regulate GABA synaptic vesicle content.

Low-affinity $GABA_A$ antagonists have an enhanced blocking effect after MeAIB application

To establish whether a decrease in the cleft transient of GABA explains the eIPSC depression induced by MeAIB, we used quickly dissociating competitive $GABA_A$ antagonists, which have been used to evaluate the kinetics of synaptic neurotransmitter transients (Clements et al., 1992). The duration of elevated GABA in the synaptic cleft after synaptic activation is dependent on the amount of GABA release by the vesicle; because weak competitive antagonists (like TPMPA) dissociate more rapidly than the typical cleft transient of GABA, their efficacy is very sensitive to initial cleft GABA concentration. If less GABA is released, then the neurotransmitter cleft transient should also be reduced in duration, and the IPSC blockade by TPMPA would be enhanced. To conduct this analysis, we compared the effects of the competitive low- and high-affinity $GABA_A$ antagonists, TPMPA (Jones et al., 2001) and gabazine, respectively, in the presence of MeAIB before and after burst stimulation. To maximize the probability of measuring changes in the effects of these antagonists, an optimal blocking concentration that produces ~20% eIPSC blockade in basal conditions was first determined (TPMPA, 30 μM; gabazine, 30–60 nM). The effects of these low concentrations of antagonists were then compared with the activity of the antagonist after burst stimulation. The selected antagonists were washed on (>10 min) and off (>20–30 min) completely before and after burst stimulation (Fig. 5A). This was assessed by establishment of a stable blocking effect of the antagonist for wash in and recovery to preantagonist eIPSC amplitude after washout. After stimulation in the presence of MeAIB, eIPSCs became smaller, and TPMPA blockade of IPSCs increased to 183 ± 50% of preburst levels

(from 12.5 ± 2.3 to 30.1 ± 3.2% block, prestimulation and poststimulation, respectively; $p < 0.005$; $n = 6$) (Fig. 5B,C) consistent with a reduction in the cleft transient of GABA. As expected, there was no change in the high-affinity blockade of eIPSCs by gabazine (Fig. 5D) (from 21.6 ± 5 to 19.6 ± 7% block, prestimulation and poststimulation, respectively; $p = 0.59$; $n = 4$). These results provide direct evidence that MeAIB-induced reductions in eIPSC amplitude are accompanied by a decrease in the cleft transient of GABA, which is consistent with a decrease in GABA vesicle content.

Minimal stimulation-evoked IPSCs demonstrate activity-dependent potency reductions after disruption of glutamate-glutamine cycle

Although the above pharmacologic experiments demonstrate that the glutamate-glutamine cycle is necessary to maintain IPSC size, changes in eIPSC amplitude after moderate stimulation in the presence of glutamate-glutamine cycle blockers involve at least two factors: increase in probability of release and decrease in postsynaptic currents. To isolate changes in synaptic currents from changes in probability of release, as well as other factors potentially inherent in synchronously activating large numbers of GABAergic terminals, we observed more quantal events such as mIPSCs. However, as we have demonstrated, mIPSCs and sIPSCs are not affected by disruption of the glutamate-glutamine cycle. Therefore, we measured the effect of moderate stimulation on meIPSCs.

meIPSCs were generated by stimulation administered using a patch pipette placed near the proximal dendrite of a recorded CA1 pyramidal cell. To select the appropriate stimulus intensity necessary to evoke the small, all-or-none events characteristic of minimal stimulation-evoked synaptic currents, the stimulus intensity was titrated from 10 to 20 μA to find a stimulus level producing approximately equal numbers of meIPSCs and failures (Fig. 6A). The other important requirement in these studies was that the synapse generating the meIPSC also had to be activated by the moderate stimulation protocol (which was administered by a large, bipolar stimulating electrode). This was tested using a paired-pulse protocol similar to that in Figure 3, and shown in Figure 6B, in which evoking the large eIPSC caused a significant increase in the number of failures in the meIPSC responses, evoked 100 ms later.

This allowed us to measure changes in the synaptic current and changes in probability of release separately. Under control conditions, the averaged meIPSC size was increased after burst stimulation (to 169 ± 14% of prestimulus levels; $p < 0.05$; $n = 4$) (Fig. $7A_2$); this was similar to the eIPSC results described above and in Figure 2, demonstrating that the quantal meIPSCs targeted by our stimulation protocol were altered in a similar manner to the compound response making up the larger eIPSCs. Yet, there was no significant change under control conditions in the size of meIPSCs excluding failures (i.e., potency) after the stimulation protocol (increase to 117 ± 20%; $p = 0.39$; $n = 4$) (Fig. $7A_1,A_3$). Consistent with the paired-pulse data in Figure 3, there was a decrease in the number of failures in each record (39 ± 14% increase in ratio of events to total trials; $p < 0.03$; $n = 4$) (Fig. $7A_3$). Together, these data strongly suggest that, after the stimulation protocol under control conditions, the increase in eIPSC size is almost completely dependent on the increase in the probability of release (Fig. $7A_1$–A_3).

If the MeAIB-induced eIPSC reduction after the stimulation protocol is attributable to a decrease in quantal currents, then we would expect this to be reflected in the averaged meIPSCs and,
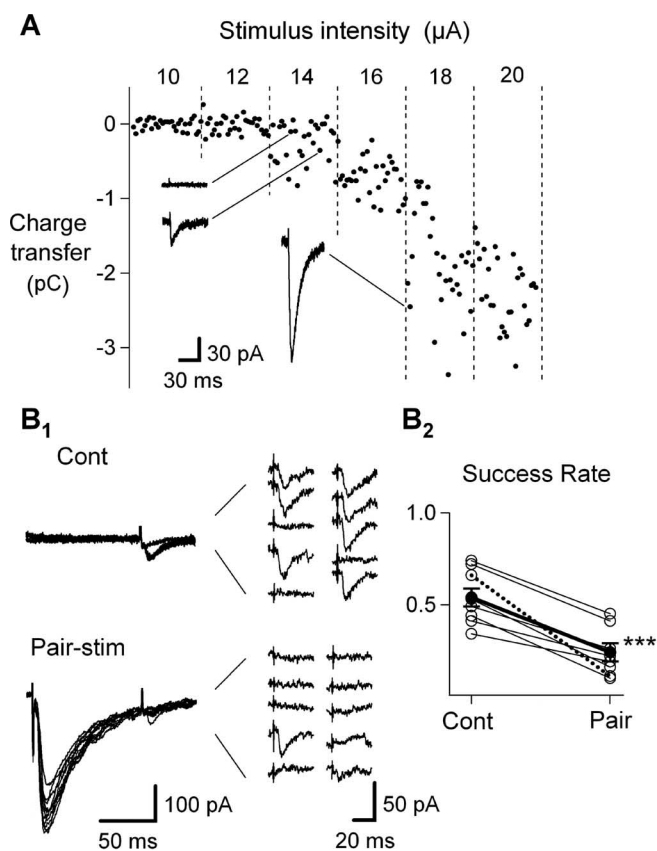
A

Figure 6. Recording and analysis of meIPSCs. ***A***, To determine an appropriate stimulus intensity to elicit meIPSCs, a set of evoked IPSCs is activated by titrating stimulus intensities (administered through a patch electrode) to find small all-or-none events. This titration is illustrated as an increase in the charge transfer of each event (●) from failures at 10 and 12 μA, to no failures and predominantly large events (>100 pA; inset) at stimulus intensities >16 μA. Within a narrow range of stimulus intensities, in this case 14 μA, a mixture of failures and small (30 pA; inset) all-or-none events characteristic of meIPSCs are generated. ***B₁, B₂*** To determine that the meIPSC response is from a synapse activated during the moderate stimulus protocol (driven by an alternate large bipolar stimulating electrode), the meIPSC was preceded 100 ms by the eIPSC (Pair-stim) as described in Materials and Methods, and a change in success rate (compared with meIPSC stimuli alone; Cont) was assessed to determine whether the two stimuli interacted. Ten control responses and paired stimuli are overlayed and expanded in ***B₁*** and clearly show a decrease in successful responses in the pairing protocol. ***B₂***, This was true for each cell used in the experiments in Figure 7 (thick line is averaged effect for 8 cells; dotted line shows cell in ***B₁***). ***p < 0.0003.

because of an expected decrease in failures, to an even greater extent in potency. This was the case. Although there was a similar increase in probability of release in both control and MeAIB conditions after moderate stimulation (30 ± 12% increase in meIPSC occurrence; $p < 0.04$; $n = 4$) (Fig. 7B_3), there was a marked decrease in potency (to 55 ± 8% of control; $p < 0.03$; $n = 4$) (Fig. 7B_1,B_3) and a more modest reduction in average meIPSCs (including failures, to 64 ± 14% of control; $n = 4$) (Fig. 7B_2). The potency data also underestimates the actual effect on synaptic inhibition, because it was necessary to collect events over 15 min after the moderate stimulation to obtain an adequate sample for analysis (180 events), by the end of which time the IPSC reduction had begun to recover (compare Fig. 2). Together, these data suggest that modulation of the glutamate-glutamine cycle could have a major impact on inhibition, and that reductions in substrate availability at any point in the glutamate-glutamine cycle may elicit a complex, dynamic modulation of inhibition under physiologic conditions.

The glutamate-glutamine cycle dynamically regulates IPSCs evoked by physiological activity patterns

In a final set of experiments, we examined how the glutamate-glutamine cycle may contribute to sculpting and maintaining inhibitory synaptic efficacy during *in vivo* patterns of activation. To do this, we created two 10 s duration stimulation protocols derived from patterns of spike activity recorded from an inhibitory basket cell in area CA1 in an unanaesthetized rat during both sleep and waking periods (provided by Dr. Gyorgy Buzsaki, Rutgers University). Using these activity patterns to drive our stimulator, we recorded eIPSCs activated in response to the high-activity, sleep recording (Fig. 8*A*) and the low-activity, waking recording (Fig. 8*B*). Activation frequency during the sleep stimulus was high, exceeding 200 Hz during brief bursts (Fig. 8*A₁*) and was low during the waking recording, averaging <1 Hz (Fig. 8*B₁*). eIPSCs were variable during the course of either stimulus protocol. This was particularly true for the sleep stimulus, in which large synaptic responses were only maintained for the first few seconds of stimulation, followed by a long periods of sustained eIPSCs, which were 5–20% of control amplitudes (Fig. 8*A₁,A₃*). However, response amplitudes to individual stimuli were similar from trial to trial. Repeated administration of either the sleep or wake stimulus protocol elicited similar responses to each repetition (data not shown), as has been described for analogous experiments using natural activity patterns examining Schaffer collateral synaptic responses (Dobrunz and Stevens, 1999).

What role could the glutamate-glutamine cycle play in regulating inhibitory synaptic responses in response to real activity patterns? To begin to answer this question, we compared responses to sleep and wake stimulus trains in the presence and absence of MeAIB. MeAIB was chosen over MSO, because it acts extracellularly to block System A transporters, and its effects are rapidly reversible. Blockade of the glutamate-glutamine cycle had complex actions on sleep responses, particularly during burst activation (Fig. 8*A₂*). The summed effect was to reduce charge transfer by 52% over the course of the stimulus train relative to controls (Fig. 8*A₃*), but individual eIPSCs were modulated differentially, based on the short (tens of milliseconds) and medium (seconds) term history of activation of the synapse. At a short time scale, eIPSCs occurring early during a high-frequency burst were only slightly reduced, whereas eIPSCs occurring later in a burst were reduced by 80–90% (Fig. 8*A,a,b*). This MeAIB effect on sleep patterns of activation contrasted significantly to those seen on low-frequency, wake patterns of activation (Fig. 8*B₁*), in which little effect was evident, with total charge transfer only being marginally (16%) reduced on average (Fig. 8*B₂*). These data demonstrate that the glutamate-glutamine cycle is critical in maintaining inhibitory synaptic efficacy and is involved both on a very short and long time scale. Responses occurring late during a single burst of activation lasting only 20–40 ms can be reduced by 80–90% by interfering with glutamate uptake, whereas sustained responses can be reduced almost to the point of failure by protracted block of the glutamate-glutamine cycle (Fig. 8*A₂c*). Thus, normal GABAergic synaptic efficacy appears to be dependent on the ability of the astrocytes to generate glutamine from extracellular glutamate, paired with the ability of the GABAergic neuron to transport that glutamine into GABAergic terminals, where it can serve as a substrate for local GABA generating pathways.

Discussion
Our results demonstrate that the astrocytic glutamate-glutamine cycle plays a crucial role in maintaining synaptic release of GABA
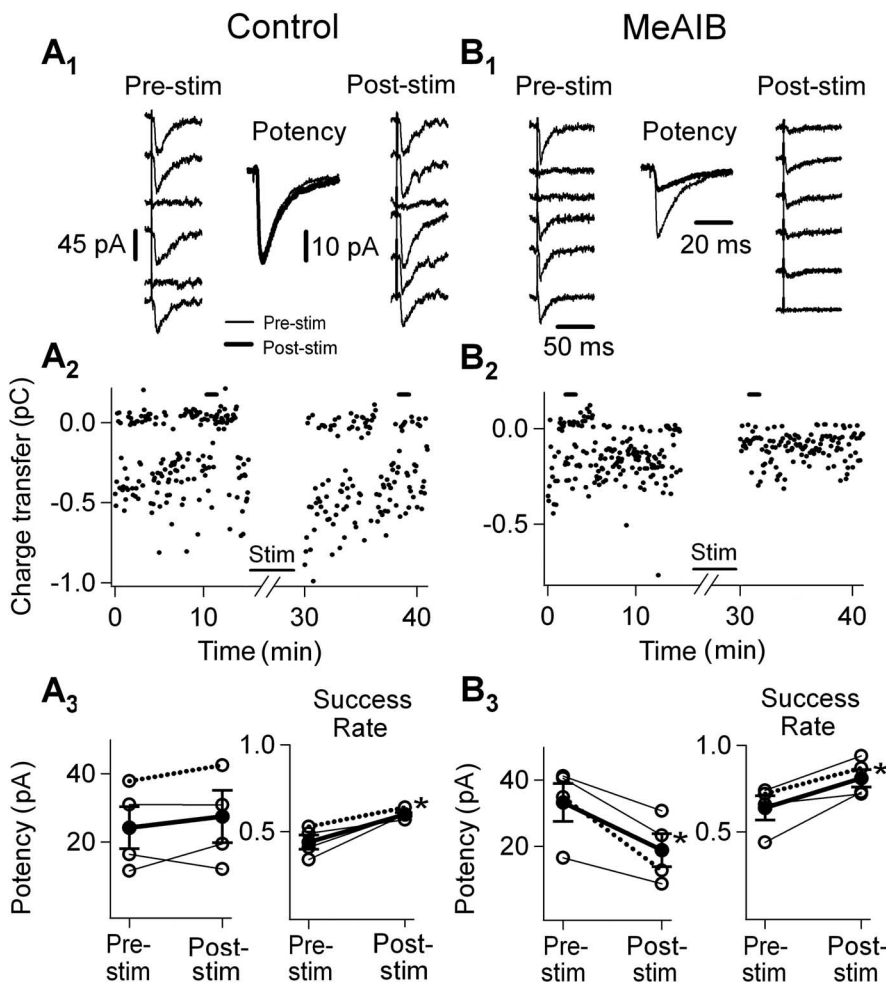
Figure 7. meIPSCs are sensitive to disruption of the glutamate-glutamine cycle by MeAIB. A_1, Consistent with an increase in eIPSC size caused by an increase in probability of release, meIPSCs under control conditions showed no change in potency and a reduction in failures after the burst stimulation protocol. This is illustrated by the lack of change comparing the events evoked preceding the moderate stimulation (Pre-stim; left) to events after the stimulation (Post-stim; right), and by a decrease in the number of failures post-stim (right). The inset (potency) depicts the average potency (event size excluding failures) before (thin line; mean of 91 events) and after (thick line; 102 event) stimulation. A_2 plots the event area versus stimulus time for the cell depicted in A_1. Note that events are all-or-none and that there is no change in event area for successes after stimulation but a decrease in failures (evident as a decrease in 0 pC events). A_3, Plot of change in potency and success rate of individual cells ($n = 4$) before and after the burst stimulation protocol. Average effect is plotted by the thick line, $\pm$ SEM. Note that there is no change in potency but a significant increase in success rate (decreased failures; $p < 0.03$) after stimulation. B_1, Consistent with a decrease in eIPSC size because of a decrease in GABA release, meIPSCs under 5 mM MeAIB-exposed conditions exhibited a decrease in potency (mean of 128 events pre-stim and 149 events post-stim) and an increased probability of release after the burst stimulation protocol. This is illustrated by the reductions evident comparing the events evoked preceding the moderate stimulation (Pre-stim; left) to events after the stimulation (Post-stim; right), and by a decrease in the number of failures post-stim (right). The inset (potency) depicts the average potency (event size excluding failures) before (thin line) and after (thick line) stimulation protocol. B_2 plots the event area versus stimulus time for the cell depicted in B_1. Note that events are all-or-none and that there is a reduction in event area for successes after stimulation and a decrease in failures (evident as a decrease in 0 pC events). B_3, Plot of change in potency and success rate of individual cells ($n = 4$) before and after the burst stimulation protocol. Average effect is plotted by the thick line, $\pm$ SEM. Note that there is a significant decrease in potency ($p < 0.03$) and a significant increase in success rate (decreased failures; $p < 0.04$) after stimulation.

neurons. Assaying changes in cleft GABA transients at stimulated synapses with a low-affinity antagonist demonstrated that the reduced synaptic efficacy was attributable to reduced GABA release. This was further corroborated in meIPSC studies, where it was demonstrated that synaptic potency was significantly reduced by MeAIB application in active synapses. Furthermore, studies with antagonists directed at various proteins in the glutamine-glutamate cycle demonstrate that glutamine used to synthesize GABA is predominantly derived from astrocytes, and furthermore that glutamine synthesis in astrocytes appears to be in turn dependent on the availability of extracellular glutamate. This may constitute an astrocytic mechanism to directly couple circuit activity levels with inhibitory efficacy. This is the first direct demonstration that the astrocytic glutamate-glutamine cycle serves as an endogenous mechanism that dynamically regulates GABAergic synaptic strength under physiological conditions.

Presynaptic GABA is regulated by synaptic activity
Several recent studies have demonstrated that synaptic strength can be modulated by experimentally altering neurotransmitter content of vesicles, without changing synaptic vesicle volume, probability of release, or the size of the readily releasable pool (Van der Kloot et al., 2000; Zhou et al., 2000; Engel et al., 2001; Van der Kloot et al., 2002). Our data suggest that regulation of synaptic strength by alteration of synaptic GABA release occurs naturally in synapses during physiologic levels of activity. Thus, the glutamate-glutamine cycle acts as a reserve mechanism that supplies metabolic precursors for GABA synthesis locally to active synapses. Interruption of this cycle at any point rapidly decreases inhibitory synaptic efficacy at active synapses. Therefore, intrinsic factors regulating the astrocytic glutamate-glutamine cycle may represent novel mechanisms of synaptic plasticity that may be important under normal and/or pathological conditions.

in active inhibitory synapses. The effects of blockade of the glutamate-glutamine cycle were tested after multiple stimulus patterns, including *in vivo* patterns of basket cell firing in area CA1 of a behaving rat. Blockade of the glutamine-glutamate cycle reduced both eIPSC and meIPSC amplitudes, without changing release probability or postsynaptic GABA receptor sensitivity at affected synapses. The effects of glutamate-glutamate cycle blockers were activity dependent and specific. No change in synaptic efficacy was evident in unstimulated synapses in the same

Blockade of either glutamine transport or synthesis had no effect on spontaneous IPSCs but significantly decreased eIPSCs in active synapses
The neuronal System A transporter is expressed at high levels in hippocampal area CA1, where it is the dominate neuronal glutamine uptake mechanism, sustaining the glutamate-glutamine cycle (Chaudhry et al., 2002a,b). Blockade of glutamine transport or inhibition of glutamine synthesis had no effect on mIPSC amplitudes, suggesting that, in low-activity conditions, glu-

tamine has little or no role in regulating synaptic GABA levels. Alternate mechanisms, such as neuronal glutamate uptake (e.g., through EAAC1) and the other sources of GABA (e.g., GAT-1-mediated direct GABA recycling), are likely to be the predominant contributors in maintaining the synaptic pool of neurotransmitter under these conditions. This hypothesis is in agreement with the finding that either treatment of animals with EAAC1 antisense oligonucleotides or blockade of glutamate uptake into inhibitory presynaptic terminals decreased mIPSC amplitudes recorded from CA1 neurons (Sepkuty et al., 2002; Mathews and Diamond, 2003). However, when synapses are functioning normally, an enhanced supply of GABA is required, because vesicles are being released and refilled in an ongoing manner.

Little is known about what, under normal conditions, is the relative contribution of intraterminal uptake of glutamate and recycling of GABA to the ongoing refilling of GABA vesicles in inhibitory synapses. Data from recent studies in GABA synaptosomes demonstrated that the vesicular GABA transporter, which transports GABA from the terminal cytoplasm into the vesicle lumen, forms a protein complex with GAD (Jin et al., 2003). Therefore, newly synthesized GABA may serve as a preferred source of transmitter to be packaged into GABA vesicles, whereas recycled GABA may constitute a secondary source. This would suggest that increased GAD activity would necessarily accompany an elevation of inhibitory neuronal activity, whereas our data suggest that the glutamate-glutamine cycle plays a prominent role in supplying glutamate as a precursor for GABA synthesis in inhibitory terminals.

Our studies provide evidence that the glutamate-glutamine cycle is an important determinant of the ability of inhibitory synapses to maintain synaptic vesicle content of GABA, regulating efficacy during sustained periods of activity. Vesicle content is not static. It reflects a dynamic equilibrium, which depends on the bidirectional flux of transmitter molecules into and out of the vesicle. Flux kinetics are determined both by transmitter concentration in the vesicle and in the synaptic terminal cytoplasm. Thus, vesicle content at equilibrium reflects the dynamics of filling and leak, both of which depend on the concentration of neurotransmitter (Williams, 1997; Axmacher et al., 2004). Depleting or enhancing cytoplasmic concentrations of neurotransmitter would therefore be expected to decrease or enhance vesicle content, respectively, as has been observed experimentally in various synapses (cf. Murphy et al., 1998; Pothos et al., 1998), including hippocampal inhibitory synapses (Engel et al., 2001; Sepkuty et al., 2002; Mathews and Diamond, 2003). We hypothesize that interference with the glutamate-glutamine cycle during periods of sustained activity decreases terminal cytoplasm concentrations of glutamate, which in turn reduces vesicle content of GABA by
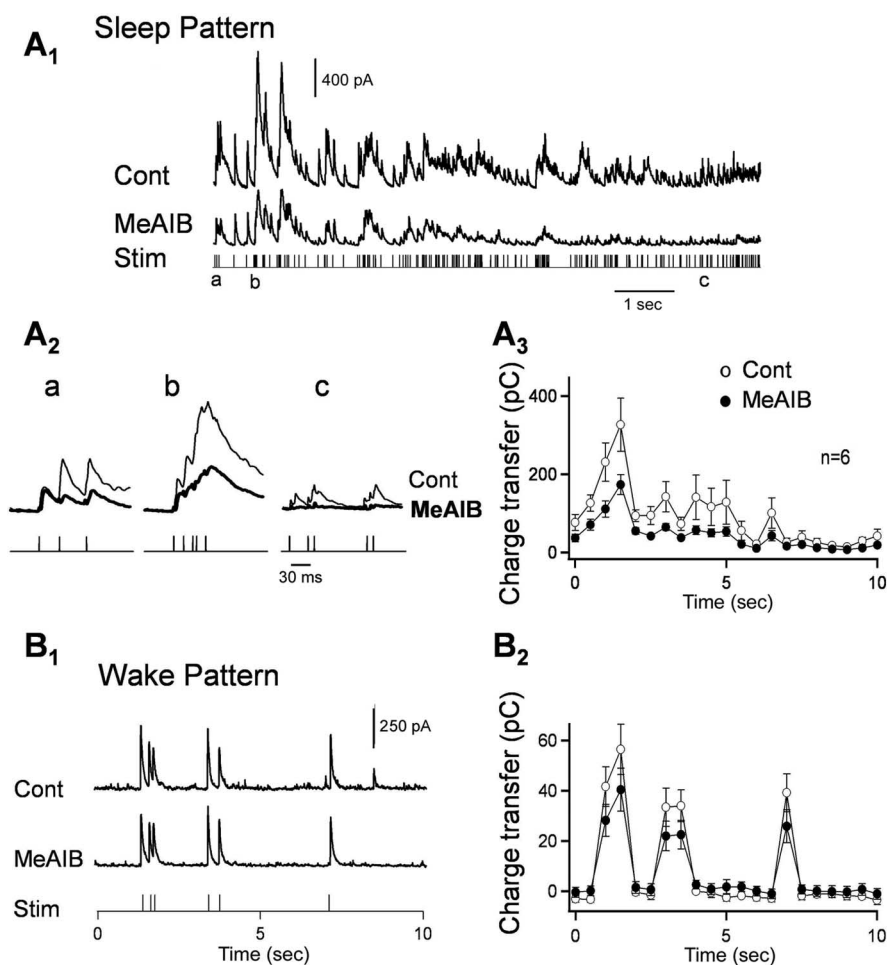

Figure 8. Natural stimulus patterns reveal multiple interactions between stimulus train frequency and glutamine availability, which in turn regulate inhibitory efficacy. We used two stimulus patterns recorded *in vivo* from a putative inhibitory basket cell, one from a period of high heterogeneous activity, including bursting over 200 Hz, recorded during sleep and another pattern of low activity recorded when the animal was awake. Ten seconds of representative traces induced by the sleep period are shown in *A₁*, evoked in either control conditions (Cont; top) or in the presence of the glutamine uptake blocker MeAIB (5 mM; below); the stimulation (Stim) pattern is presented under both. Traces in *A₂* show at higher resolution that, compared with controls, there is both an intraburst reduction in IPSCs in 5 mM MeAIB (*a*, *b*) occurring over the millisecond time scale as well as a more general reduction incurred over seconds (*c*). Reduced eIPSC size is also reflected in *A₃* as a significant decrease in charge transfer when MeAIB and control conditions are compared at 500 ms intervals in six cells. In contrast, in *B₁* and *B₂*, there appears to be very little effect of MeAIB on GABAergic synapses stimulated with the wake pattern in the representative trace (*B₁*), which is also evident in the mean group charge transfer data (*B₂*) plotted from the same six cells shown in *A₃*.

altering both the dynamics of vesicle recycling (refilling rate) and the GABA content of "resting" vesicles. Depletion of neurotransmitter content of "resting" GABA vesicles has been demonstrated experimentally, after blockade of neuronal glutamate uptake (Mathews and Diamond, 2003). A recent study has shown that hippocampal inhibitory synapses exhibit little or no "kiss and run" release (Li et al., 2005). Therefore, the reduced efficacy of both eIPSCs and meIPSCs seen after interference with the glutamate-glutamine cycle (Figs. 2, 7) is consistent with a reduction in neurotransmitter content.

Normal and pathological factors modulating the glutamate-glutamine cycle

Given the functional importance of the glutamate-glutamine cycle in regulating inhibitory synaptic efficacy, activity-dependent, or pathology-dependent regulation of enzymes and transporters important in the generation of glutamine could be a powerful mechanism to modulate circuit excitability. We have demon-

strated that interrupting glutamate uptake in astrocytes, synthesis of that glutamate into glutamine, and transport of glutamine from astrocytes into GABAergic neurons can all profoundly reduce inhibitory efficacy. Each of these points in the cycle are also targets of regulation.

Reduced expression of glial glutamate transporters is associated with a number of neurodegenerative diseases (for review, see Maragakis and Rothstein, 2004). Excitotoxicity caused by increases in ambient glutamate is often the posited mechanistic link between reduced uptake and pathology, but our data suggest that the contribution of disinhibition resulting from lack of glutamine production should also be considered.

Glutamine synthetase is also a target for modulation. The glutamine synthetase promoter contains a nuclear factor κB (NF-κB) responsive element, which suggests that glutamine synthetase expression may be upregulated in response to CNS injuries, which induce expression of NF-κB (Belin et al., 1997). Glucocorticoids have also been shown to increase glutamine synthetase mRNA expression in Muller cells (Gorovits et al., 1994; Grossman et al., 1994), and this can be repressed by c-Jun protein (Vardimon et al., 1999), or REST binding to the neuronal restrictive silencer element in the glutamine synthetase promoter (Avisar et al., 1999). Moreover, NMDA receptor activation modulates glutamine synthetase activity and glutamine content in brain *in vivo* (Kosenko et al., 2003). Glutamine production is also perturbed in pathological conditions. For example, patients with schizophrenia or mesial temporal lobe epilepsy both exhibit decreased glutamine synthetase expression in astrocytes (Burbaeva et al., 2003; Eid et al., 2004).

The glutamate-glutamine cycle, in addition to being regulated at the level of glutamate transport and glutamine synthesis, may also be modulated by changes in glutamine transport. Glutamate application to cultured astrocytes increases SN-1-mediated (astrocytic) glutamine transport activity (Broer et al., 2004). Neuronal (System A) glutamine transport may also be regulated, because an increasing abundance of the SA-2 subtype (SAT2) mRNA and protein has been demonstrated after amino acid deprivation and/or exposure of cells to a hypertonic environment in a variety of cultured cell lines (McGivan and Pastor-Anglada, 1994; Franchi-Gazzola et al., 2001; Hyde et al., 2001; Alfieri et al., 2005).

Thus, as befitting a pathway that during periods of sustained activity *in vivo* potentially contributes over half the synaptic GABA, the glutamate-glutamine cycle appears to have multiple avenues for regulation. Because astrocyte membrane is found to be interdigitated in both synaptic and extrasynaptic space, and that membrane is responsible for at least 80% of the glutamate clearance and the majority of synaptic inactivation in the brain (Bergles and Jahr, 1997; Danbolt, 2001), glutamate is poised to directly and locally link excitatory activity to inhibitory output by modulating GABAergic synaptic strength under physiological conditions.

References

Alfieri RR, Bonelli MA, Petronini PG, Desenzani S, Cavazzoni A, Borghetti AF, Wheeler KP (2005) Hypertonic stress and amino acid deprivation both increase expression of mRNA for amino acid transport system A. J Gen Physiol 125:37–39.

Arriza JL, Fairman WA, Wadiche JI, Murdoch GH, Kavanaugh MP, Amara SG (1994) Functional comparisons of three glutamate transporter subtypes cloned from human motor cortex. J Neurosci 14:5559–5569.

Avisar N, Shiftan L, Ben-Dror I, Havazelet N, Vardimon L (1999) A silencer element in the regulatory region of glutamine synthetase controls cell type-specific repression of gene induction by glucocorticoids. J Biol Chem 274:11399–11407.

Axmacher N, Stemmler M, Engel D, Draguhn A, Ritz R (2004) Transmitter metabolism as a mechanism of synaptic plasticity: a modeling study. J Neurophysiol 91:25–38.

Bartos M, Vida I, Frotscher M, Meyer A, Monyer H, Geiger JR, Jonas P (2002) Fast synaptic inhibition promotes synchronized gamma oscillations in hippocampal interneuron networks. Proc Natl Acad Sci USA 99:13222–13227.

Belin MF, Didier-Bazes M, Akaoka H, Hardin-Pouzet H, Bernard A, Giraudon P (1997) Changes in astrocytic glutamate catabolism enzymes following neuronal degeneration or viral infection. Glia 21:154–161.

Bergles DE, Jahr CE (1997) Synaptic activation of glutamate transporters in hippocampal astrocytes. Neuron 19:1297–1308.

Bjoras M, Gjesdal O, Erickson JD, Torp R, Levy LM, Ottersen OP, Degree M, Storm-Mathisen J, Seeberg E, Danbolt NC (1996) Cloning and expression of a neuronal rat brain glutamate transporter. Brain Res Mol Brian Res 36:163–168.

Broer A, Deitmer JW, Broer S (2004) Astroglial glutamine transport by system N is upregulated by glutamate. Glia 48:298–310.

Burbaeva GS, Boksha IS, Turishcheva MS, Vorobyeva EA, Savushkina OK, Tereshkina EB (2003) Glutamine synthetase and glutamate dehydrogenase in the prefrontal cortex of patients with schizophrenia. Prog Neuropsychopharmacol Biol Psychiatry 27:675–680.

Chaudhry FA, Reimer RJ, Edwards RH (2002a) The glutamine commute: take the N line and transfer to the A. J Cell Biol 157:349–355.

Chaudhry FA, Schmitz D, Reimer RJ, Larsson P, Gray AT, Nicoll R, Kavanaugh M, Edwards RH (2002b) Glutamine uptake by neurons: interaction of protons with system A transporters. J Neurosci 22:62–72.

Clements JD, Lester RA, Tong G, Jahr CE, Westbrook GL (1992) The time course of glutamate in the synaptic cleft. Science 258:1498–1501.

Danbolt NC (2001) Glutamate uptake. Prog Neurobiol 65:1–105.

Dobrunz LE, Stevens CF (1999) Response of hippocampal synapses to natural stimulation patterns. Neuron 22:157–166.

Eid T, Thomas MJ, Spencer DD, Lai JCK, Malthankar GV, Kim JH, Danbolt NC, Ottersen OP, de Lanerolle NC (2004) Loss of glutamine synthetase in the human epileptogenic hippocampus: possible mechanism for raised extracellular glutamate in mesial temporal lobe epilepsy. Lancet 363:28–37.

Engel D, Pahner I, Schulze K, Frahm C, Jarry H, Ahnert-Hilger G, Draguhn A (2001) Plasticity of rat central inhibitory synapses through GABA metabolism. J Physiol (Lond) 535:473–482.

Eskandari S, Kreman M, Kavanaugh MP, Wright EM, Zamighi GA (2000) Pentameric assembly of a neuronal glutamate transporter. Proc Natl Acad Sci USA 97:8641–8646.

Franchi-Gazzola R, Sala R, Bussolati O, Visigalli R, Dall'Asta V, Ganapathy V, Gazzola GC (2001) The adaptive regulation of amino acid transport system A is associated to changes in ATA2 expression. FEBS Lett 490:11–14.

Gorovits R, Ben-Dror I, Fox LE, Westphal HM, Vardimon L (1994) Developmental changes in the expression and compartmentalization of the glucocorticoid receptor in embryonic retina. Proc Natl Acad Sci USA 91:4786–4790.

Grossman R, Fox LE, Gorovits R, Ben-Dror I, Reisfeld S, Vardimon L (1994) Molecular basis for differential expression of glutamine synthetase in retina glia and neurons. Brain Res Mol Brain Res 21:312–320.

Huang YH, Sinha SR, Tanaka K, Rothstein JD, Bergles DE (2004) Astrocyte glutamate transporters regulate metabotropic glutamate receptor-mediated excitation of hippocampal interneurons. J Neurosci 24:4551–4559.

Hwang TN, Copenhagen DR (1999) Automatic detection, characterization, and discrimination of kinetically distinct spontaneous synaptic events. J Neurosci Methods 92:65–73.

Hyde R, Christie GR, Litherland GJ, Hajduch E, Taylor PM, Hundal HS (2001) Subcellular localization and adaptive up-regulation of the System A (SAT2) amino acid transporter in skeletal-muscle cells and adipocytes. Biochem J 355:563–568.

Jin H, Wu H, Osterhaus G, Wei J, Davis K, Sha D, Floor E, Hsu CC, Kopke RD, Wu JY (2003) Demonstration of functional coupling between gamma-aminobutyric acid (GABA) synthesis and vesicular GABA transport into synaptic vesicles. Proc Natl Acad Sci USA 100:4293–4298.

Jones MV, Jonas P, Sahara Y, Westbrook GL (2001) Microscopic kinetics and energetics distinguish GABA(A) receptor agonists from antagonists. Biophys J 81:2660–2670.

Kanai Y, Hediger MA (1992) Primary structure and functional characterization of a high-affinity glutamate transporter. Nature 360:467–471.

Klausberger T, Magill PJ, Marton LF, Roberts JD, Cobden PM, Buzsaki G, Somogyi P (2003) Brain-state- and cell-type-specific firing of hippocampal interneurons in vivo. Nature 421:844–848.

Kosenko E, Llansola M, Montoliu C, Monfort P, Rodrigo R, Hernandez-Viadel M, Erceg S, Sanchez-Perez AM, Felipo V (2003) Glutamine synthetase activity and glutamine content in brain: modulation by NMDA receptors and nitric oxide. Neurochem Int 43:493–499.

Lambert NA, Wilson WA (1994) Temporally distinct mechanisms of use-dependent depression at inhibitory synapses in the rat hippocampus in vitro. J Neurophysiol 72:121–130.

Li Z, Burrone J, Tyler WJ, Hartman KN, Albeanu DF, Murthy VN (2005) Synaptic vesicle recycling studied in transgenic mice expressing synapto-pHluorin. Proc Natl Acad Sci USA 102:6131–6136.

Martin DL, Tobin AJ (2000) Mechanisms controlling GABA synthesis and degradation in the brain. In: GABA in the nervous system (Martin DL, Olsen RW, eds), pp 25–41. Philadelphia: Lippincott Williams & Wilkins.

Mathews G, Diamond J (2003) Neuronal glutamate uptake contributes to GABA synthesis and inhibitory synaptic strength. J Neurosci 23:2040–2048.

Maragakis NJ, Rothstein JD (2004) Glutamate transporters: animal models to neurologic disease. Neurobiol Dis 15:461–473.

McGivan JD, Pastor-Anglada M (1994) Regulatory and molecular aspects of mammalian amino acid transport. Biochem J 299:321–334.

Murphy DD, Cole NB, Greenberger V, Segal M (1998) Estradiol increases dendritic spine density by reducing GABA neurotransmission in hippocampal neurons. J Neurosci 18:2550–2559.

Nakayama T, Kawakami H, Tanaka K, Nakamura S (1996) Expression of three glutamate transporter subtype mRNAs in human brain regions and peripheral tissues. Brain Res Mol Brain Res 36:189–192.

Perez Y, Chapman CA, Woodhall G, Robitaille R, LaCaille JC (1999) Differential induction of long-lasting potentiation of inhibitory postsynaptic potentials by theta patterned stimulation versus 100-Hz tetanization in hippocampal pyramidal cells in vitro. Neuroscience 90:747–757.

Pines G, Danbolt NC, Bjoras M, Zhang Y, Bendahan A, Eide L, Koepsell H, Strom-Mathisen J, Seeberg E, Kanner BI (1992) Cloning and expression of a rat brain L-glutamate transporter. Nature 360:464–467.

Pothos EN, Davila V, Sulzer D (1998) Presynaptic recording of quanta from midbrain dopamine neurons and modulation of the quantal size. J Neurosci 18:4106–4118.

Rae C, Hare N, Bubb WA, McEwan SR, Broer A, McQuillan JA, Balcar VJ, Conigrave AD, Broer S (2003) Inhibition of glutamine transport depletes glutamate and GABA neurotransmitter pools: further evidence for metabolic compartmentation. J Neurochem 85:503–514.

Sepkuty J, Cohen A, Eccles C, Rafiq A, Behar K, Ganel R, Coulter D, Rothstein J (2002) A neuronal glutamate transporter contributes to neurotransmitter GABA synthesis and epilepsy. J Neurosci 22:6372–6379.

Van der Kloot W, Colasante C, Cameron R, Molgo J (2000) Recycling and refilling of transmitter quanta at the frog neuromuscular junction. J Physiol (Lond) 523:247–258.

Van der Kloot W, Molgo J, Cameron R, Colasante C (2002) Vesicle size and transmitter release at the frog neuromuscular junction when quantal acetylcholine content is increased or decreased. J Physiol (Lond) 541:385–393.

Vardimon L, Ben-Dror I, Avisar N, Oren A, Shiftan L (1999) Glucocorticoid control of glial gene expression. J Neurobiol 40:513–527.

Velaz-Faircloth M, McGraw TS, Alandro MS, Fremeau Jr RT, Kilberg MS, Anderson KJ (1996) Characterization and distribution of the neuronal glutamate transporter EAAC1 in rat brain. Am J Physiol 270:C67–C75.

Williams J (1997) How does a vesicle know it is full? Neuron 18:683–686.

Zhou Q, Petersen CCH, Nicoll RA (2000) Effects of reduced vesicular filling on synaptic transmission in rat hippocampal neurons. J Physiol (Lond) 525:195–206.